OPTICAL PHONONS IN SOME VERY THIN II-VI COMPOUND FILMS

I. Giaever and H. R. Zeller
General Electric Research and Development Center, Schenectady, New York
(Received 2 October 1968)

We have used electron tunneling to determine the longitudinal optical (LO) phonons in thin films of CdS, CdO, Zns, and ZnO. The II-VI compounds were used as a tunneling barrier separating two metal films, and in some instances they were no more than 10-30 Å thick. The LO-phonon energies obtained in the various compounds agree very well with the values that have been obtained from Raman scattering and infrared spectroscopy on bulk materials.

Jaklevic and Lambe[1] have shown in a nice and convincing experiment that it is possible to obtain the molecular vibrational spectra of hydrocarbons using electron tunneling. The hydrocarbon molecules are adsorbed on the insulating layer in a tunnel junction and the vibrational modes are excited directly by the tunneling electrons. This increases the conductivity of the junctions at applied voltages which correspond to the resonant frequencies of the hydrocarbons.[2] Since the conductivity steps are small, they are most easily detected by plotting the first or second derivative of the current I with respect to the voltage V as a function of the voltage. This discovery of Jaklevic and Lambe led to the suggestion that it should be possible to excite normal modes in the barrier itself, such as phonons and magnons.[3] Indeed, Rowell[4] has tentatively identified various peaks in the second derivative curves in a Pb-PbO-Pb junction as reflecting the phonon spectrum in PbO. Of course it is known from tunneling experiments in p-n junctions,[5] in metal-semiconductor junctions,[6] and also in superconducting tunneling junctions[7] that a small structure in the current-voltage curves reflects the electron-phonon interactions in the electrodes. We emphasize that in the present experiments where we have prepared insulating barriers of II-VI compounds, we are able to separate the excitations in the barrier from the excitations in the electrodes. Because the optical phonon spectra for some of the barriers we have used are known from Raman scattering on single crystals,[8,9] we are able to establish clearly that the electrons interact with the phonons in the barrier itself.

The CdS and ZnS barriers were prepared by first evaporating a thin layer of the appropriate substance onto a freshly evaporated metal film. Because thin CdS and ZnS films contain pinholes, it is necessary that the substrate metal is allowed to oxidize after the deposition of CdS or ZnS such that an insulating oxide can form in the pinholes as previously described in some detail by one of us.[10] The junction areas used were about 1 mm^2 and the tunneling resistance in the range 10-1000 Ω. While it is possible to tunnel through an apparent thickness of a few hundred angstroms of CdS, the ZnS must be kept only a few tens of angstroms thick. We have successfully used Pb, Sn, and Al as substrate materials, as well as counter electrodes.

The CdO and ZnO junctions were prepared by simply oxidizing an evaporated film of Cd or Zn. All our films have been evaporated onto substrates kept at room temperature, and because of difficulty in getting Zn or Cd to stick to a glass slide, a very thin Al layer, less than 30 Å thick, was used to provide nucleation. The quality of the oxide layers on both Zn and Cd appeared to be a strong function of the visual appearance of the films. Films with mirrorlike appearance gave good, usable oxides, while brownish or milky appearance often resulted in shorts. Because the appearance of the film edges was poor, we found it helpful to cover them, as we suspected the edges to contribute to the number of short circuits obtained.[11] We also found it necessary to use Pb as the second electrode, as all other materials tried as counter electrodes resulted in very low resistances or short circuits. The oxides were always formed at room temperature and atmospheric pressures; the junction areas were approximately $\frac{1}{4}$ mm^2 and the resistance of the junctions in the 10- to 1000-Ω range.

The first and second derivative of the voltage with respect to the current and as a function of voltage was obtained directly by a modulation technique using a lock-in amplifier in a bridge-like circuit, constructed after a design described by Adler.[12] In order to get maximum sensitivity, peak-to-peak modulation-voltage signals as large as a few millivolts were sometimes used to obtain the second derivative while considerably less amplitude could be used for the first derivative. By using smaller voltages we could minimize signal distortion.

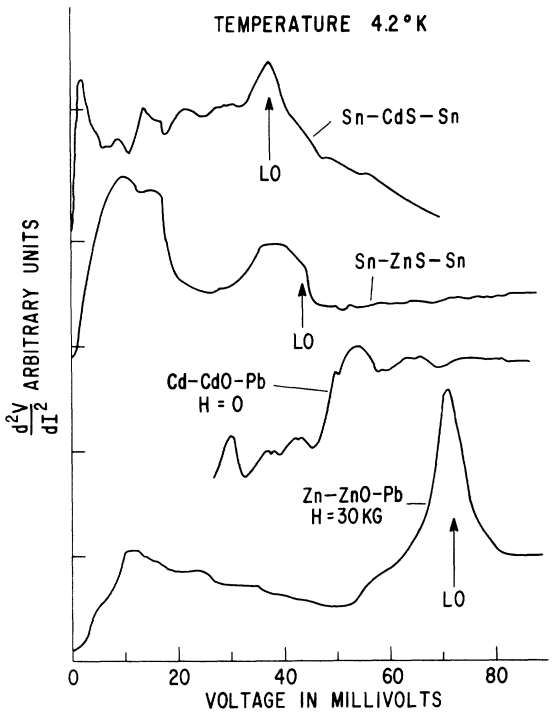

FIG. 1. d^2V/dI^2 as a function of voltage for four different barriers. The arrows indicate the position of the long-wavelength LO phonons obtained from Raman scattering data (Ref. 9).

A summary of the experimental data is shown in Fig. 1, where d^2V/dI^2 is plotted as a function of V. The longitudinal optical phonon energies available from Raman scattering are shown for comparison. As can be seen from the data the longitudinal optical phonons can be easily identified, mainly as the last rapid change in the second derivative. As seen in the curve for CdS, various peaks are also present at lower energies. Although the low-energy peaks are reproducible on any given sample and thus do not represent electrical noise, we can, in general, reproduce only the longitudinal optical phonon peaks from sample to sample. At first sight it is somewhat surprising to find approximately the same values for the energies of the optical phonons in these films and in single crystals; however, we believe that the optical phonons are in a sense closely related to molecular vibrations and relatively insensitive to crystal structure. The peaks at lower energies might be caused by phonons more sensitive to crystal structure and orientation; thus they are difficult to reproduce and indeed often absent, and little or no information can be obtained from them.

In the curve for ZnS the large peak at low voltage is caused by the phonon spectrum in the electrodes, in this case Sn. It compares well with Rowell's earlier data.[4] If Al electrodes are used, this peak is absent. The peak further out in energy is caused by the ZnS layer. The peak is rather broad as can be seen, and it is tempting to associate the onset with the TO modes which are known to be at 33 meV. An alternative explanation is to associate the width of the peak with the LO-phonon bandwidth.[13]

In the curve for CdO we do not show the data at lower voltages because at these voltages the second derivative is completely dominated by the phonon spectrum in the superconducting Pb electrode. From the curve we judge the LO-phonon energy to be at 47 meV.

The ZnO gave us the best data. Again at lower voltages the structure in the curves is associated with the phonons in the electrodes, in this case Pb and possibly Zn. The shoulder at approximately 55 meV is however always present together with the peak at 72 meV. Again from Raman scattering data it is clear that the peak at 72 meV is associated with the LO phonon, while we may attribute the shoulder at 55 meV to the TO modes, or to the bandwidth of the LO-phonon spectrum. The effect is rather large in ZnO. In Fig. 2 we show a first derivative curve, where for comparison the phonon peaks caused by superconducting Pb are also shown. The biggest resistance change which we have observed at 72 meV is approximately 1%. In Fig. 2 is also shown the second derivative for both polarities; as can be seen the shape of the characteristic is polarity dependent. Also there is a small effect as expected depending on whether the counter electrode Pb is superconducting ($H = 0$) or normal ($H = 30$ kG).

The optical-phonon spectra of all these materials are rather complex as there are nine optical and three acoustical branches in the wurtzite structure. Some of the materials are known to exist in a cubic form as well. Where the phonon spectrum has been determined by Raman scattering, well-defined single crystals have been used. However, at least in Zns the difference between the optical-phonon spectrum in the two structures is below our resolution. While the Raman scattering and infrared spectroscopy select out phonons of long wavelength, no such selection rule is known to exist for tunneling, and phonons of all wavelength should contribute to the obtained peaks. Since our barriers are indeed ill defined, i.e., we do not know the crystal structure of the films and in some instances they may even be

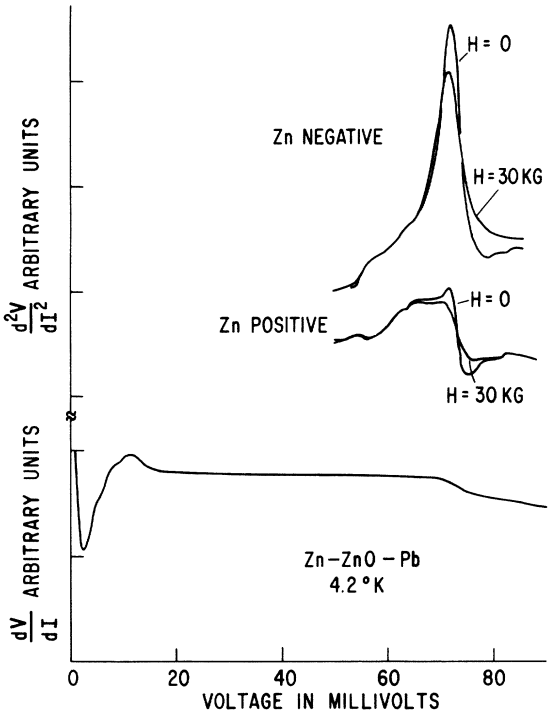

FIG. 2. The top curves illustrate the polarity dependence of a ZnO sample. A small change is also seen depending on whether the counter electrode Pb is normal ($H=0$) or superconducting ($H=30$ kG). The lower curve is a plot of dV/dI versus voltage, which compares the phonon structure at low voltages due to the superconducting Pb with the structure at 72 meV due to ZnO. The zero has been offset.

amorphous, it is somewhat surprising to us that we get such good agreement with the existing data for LO phonons of long wavelength. By and large this agreement emphasizes that the optical-phonon spectrum must depend upon short-range order rather than long-range order in the crystals. In Fig. 3 we have plotted the second derivative obtained from a 100-Å-thick Ge film sandwiched between two films of Sn. The sample is prepared similarly to the ZnS and CdS samples. As seen, the effect of the optical phonons is clearly visible in the curves; however, our structure is rather broad. Ge films prepared under our conditions are known to be amorphous, thus the broad curve can be due to bonding of various strengths. We can also interpret the width of the peaks to reflect the width of the phonon band as tunneling does not favor long-wavelength phonons.

At present these preliminary experiments clearly show that it is possible to observe some of the phonons in the barrier; however, not enough is known about the barrier itself to make detailed calculations. For example, Fig. 3 shows

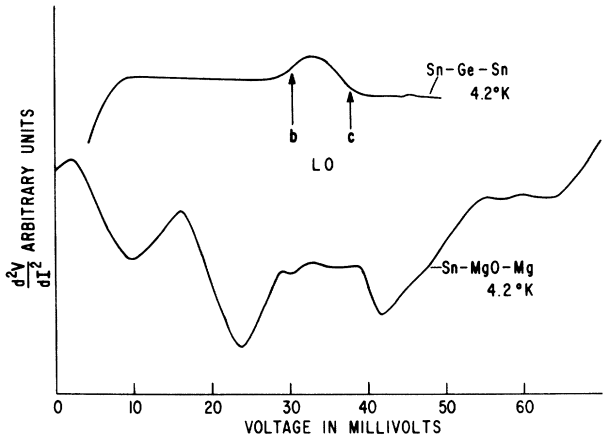

FIG. 3. d^2V/dI^2 as a function of voltage for two different barriers. The Ge barrier has been evaporated and is believed to be amorphous. The known LO-phonon energies (Ref. 13) are indicated both at the Brillouin-zone boundary, b, and at the center of the zone, c. The lower curve is for naturally grown MgO.

a plot of a Sn-MgO-Mg sandwich, and though most of this structure is reproducible between samples, we judge it at present almost impossible to interpret. Mg is known to form oxide, hydroxide, and carbonate on exposure to air and for this reason will have a rather complicated spectrum. To realize the full potential of tunneling as a probe for barrier excitations, the barriers must be better characterized than we are able to do at present. For example, epitaxial growth of barriers under high-vacuum conditions might prove very rewarding.

It is a pleasure to acknowledge the contributions of Dr. S. Roberts who generously helped in building and testing the derivative plotter.

[1]R. C. Jaklevic and J. Lambe, Phys. Rev. Letters 17, 1139 (1966).

[2]D. J. Scalapino and S. M. Marcus, Phys. Rev. Letters 18, 459 (1967).

[3]C. B. Duke, S. D. Silverstein, and A. J. Bennett, Phys. Rev. Letters 19, 312 (1967).

[4]J. M. Rowell, in Proceedings of the Advanced Study Institute on Tunneling Phenomena in Solids, Risö, Denmark (to be published).

[5]N. Holonyak, Jr., I. A. Lesk, R. N. Hall, J. J. Tiemann, and H. Ehrenreich, Phys. Rev. Letters 3, 167 (1959).

[6]F. Steinrisser, L. C. Davis, and C. B. Duke, Phys. Rev. (to be published).

[7]J. M. Rowell and L. Kopf, Phys. Rev. 137, 907 (1965).

[8]T. C. Damen, S. P. S. Porto, and B. Tell, Phys.

Rev. 142, 570 (1966).
[9]O. Brafman and S. S. Mitra, Phys Rev. 171, 931 (1968).
[10]I. Giaever, Phys. Rev. Letters 20, 1286 (1968).
[11]The "edge effect" was a controversial subject at the Advanced Study Institute on Tunneling Phenomena in Solids, Risö, Denmark. This is the first time in our experience that we have found it helpful to cover the edges; however, we do not know if it was necessary.
[12]J. G. Adler and J. E. Jackson, Rev. Sci. Instr. 37, 1049 (1966).
[13]F. A. Johnson, Progr. Semicond. 9, 181 (1965).

EXPERIMENTAL DETERMINATION OF THE EFFECTIVE ATOMIC-SCATTERING FACTOR AND RIGID-LATTICE INTERFERENCE FUNCTION IN LOW-ENERGY ELECTRON DIFFRACTION*

Max G. Lagally and Maurice B. Webb
University of Wisconsin, Madison, Wisconsin 53706
(Received 29 July 1968)

The elastic scattering of low-energy electrons from Ni is examined at temperatures where the multiphonon scattering is dominant. The effective atomic-scattering factor is extracted. The specularly reflected intensity is examined and the corrections necessary to determine the rigid-lattice interference function are discussed.

The understanding of low-energy electron diffraction is presently not satisfactory. Recently there have appeared a number of dynamical theories,[1-7] some of which extend band-structure calculations to the incident-electron energies and match wave functions at the vacuum-crystal interface, and others which treat the multiple scattering explicitly. Generally these theories either neglect inelastic processes or treat them with an adjustable parameter, use oversimplified atomic-scattering factors or lattice potentials, and consider only the rigid lattice. The experimental data are also deficient in many respects. Besides questions of real surfaces not being ideal, experimental results have not been directly comparable with theory because they have not been corrected for the diffuse scattering, the Debye-Waller factor, and the Lorentz factor. Experimental information about the atomic scattering has been available for only a few atoms, and then generally from gas data.

It is the purpose of this Letter to demonstrate a generally applicable method of measuring the square of the effective atomic-scattering factor for back angles and to present the results for Ni, to separate the specularly reflected intensity as a function of incident energy into its Bragg and diffuse components, and to illustrate several significant corrections to the Bragg intensity necessary to extract features of the rigid-lattice interference function that appears in the kinematic description of the diffraction.

We make use of the multiphonon scattering, which has been discussed previously using a kinematic description.[8,9] Although the kinematic theory is inadequate in some respects, it provides a convenient and at present the only framework in which to describe the phonon scattering. It should be emphasized that most of the results presented are meaningful independent of this theoretical description. The time-averaged intensity scattered per unit solid angle per unit incident intensity is given by

$$I(\vec{S}) = |f(\theta,E)|^2 \sum_{i,j} \exp[i\langle \vec{S}\cdot(\vec{r}_i - \vec{r}_j)\rangle] = |f(\theta,E)|^2 g(\vec{S}), \quad (1)$$

where $f(\theta,E)$ is the atomic-scattering factor, $\vec{S}=\vec{k}-\vec{k}_0$ is the diffraction vector, and $g(\vec{S})$ is the interference function. If the $\vec{r}$'s are the equilibrium atomic positions, this becomes the rigid-lattice interference function $g_0(\vec{S})$. For a thermally disordered crystal, the interference function can be separated into three parts,

$$g(\vec{S}) = g_{\text{Bragg}}(\vec{S}) + g_{\text{1-ph}}(\vec{S}) + g_{\text{m-ph}}(\vec{S}). \quad (2)$$

Its integral over the Brillouin zone is

$$\int_{\text{zone}} g(\vec{S})\,d\vec{S} = e^{-2M}[1+2M+(e^{2M}-1-2M)] \times \int_{\text{zone}} g_0(\vec{S})\,d\vec{S} = \text{const}, \quad (3)$$

where the three terms correspond to those in the interference function and $2M$ is the exponent in the Debye-Waller factor. Equation (3) was experimentally verified in Ref. 8. There it was also suggested that the multiphonon interference